

Superconductivity in $\text{SrFe}_{2-x}\text{Co}_x\text{As}_2$: Internal Doping of the Iron Arsenide Layers

A. Leithe-Jasper, W. Schnelle, C. Geibel, and H. Rosner

Max-Planck-Institut für Chemische Physik fester Stoffe, Nöthnitzer Str. 40, 01187 Dresden, Germany

In the electron doped compounds $\text{SrFe}_{2-x}\text{Co}_x\text{As}_2$ superconductivity with T_c up to 20 K is observed for $0.2 \leq x \leq 0.4$. Results of structure determination, magnetic susceptibility, electrical resistivity, and specific heat are reported. The observation of bulk superconductivity in all thermodynamic properties – despite strong disorder in the Fe-As layer – favors an itinerant picture in contrast to the cuprates and renders a p - or d -wave scenario unlikely. DFT calculations find that the substitution of Fe by Co ($x \geq 0.3$) leads to the suppression of the magnetic ordering present in SrFe_2As_2 due to a rigid down-shift of the Fe- $3d_{x^2-y^2}$ related band edge in the density of states.

PACS numbers: 74.10.+v, 74.25.Bt, 74.25.Dw

The observation of superconductivity in layered Fe-As systems has recently attracted considerable interest. The undoped compounds, e.g., LaFeAsO [1, 2] or AFe_2As_2 ($A = \text{Ba}, \text{Sr}$) [3, 4, 5], present an antiferromagnetic (afm) transition related to a structural transition at temperatures in the range 140 K to 205 K. Upon doping both the structural and the magnetic ordering get suppressed and superconductivity with T_c up to 56 K appears [1, 6, 7]. The onset of superconductivity at the disappearance of an afm ordered state induced by charge doping from a reservoir layer is reminiscent of the behavior observed in the cuprates. Since furthermore Fe and Cu are both $3d$ elements, and because of similarities in the structure of the layers, an analogy between the high temperature superconductivity (HTSC) in the cuprates and the layered Fe-As systems was suggested in a large number of reports. On the other hand, the absence of a Mott-insulator transition as well as the small ordered Fe moment in the undoped compounds put this analogy into question, and suggest that a model based on itinerant and weakly correlated $3d$ electrons might be more appropriate.

One way to get deeper insight into these questions is a doping experiment on the Fe site. Presently, doping is generally performed on sites in-between the Fe-As layers, either on the R -site or the O -site in the $R\text{FeAsO}$ systems or on the A site in the AFe_2As_2 compounds. Such kind of doping corresponds, both in a localized and in an itinerant model, to a simple charge doping and is therefore not very suitable for discriminating between both models. On the other hand, replacing a small amount of Fe by another $3d$ element should lead to different effects depending on the model used. In an itinerant model, within a simple rigid-band approach, substitution on the Fe site is expected to be quite similar to indirect doping via the interlayer sites, since only the total number of electrons is relevant. In a picture with localized $3d$ electrons, doping on the Fe site should lead to a very different behavior, since the correlations in the $3d$ layers are directly affected – a few percent Ni or Zn doping on the Cu site in a HTSC cuprate lead to a drastic reduction of T_c .

Therefore, we investigated thermodynamic properties and electrical conductivity of the solid solution

$\text{SrFe}_{2-x}\text{Co}_x\text{As}_2$. While pure SrFe_2As_2 undergoes a lattice distortion and afm ordering at $T_0 = 205$ K [4], a small amount of Co substitution leads to a rapid decrease of T_0 , followed by the onset of superconductivity in the concentration range $0.2 \leq x \leq 0.4$ with a maximum T_c of ≈ 20 K. The observation of superconductivity in Co substituted SrFe_2As_2 provides strong evidence that an analogy with the HTSC cuprates is not really justified. We therefore performed band structure calculations and discuss the electronic structure in view of our experimental results. The good agreement between calculations and experimental observations confirms that an itinerant approach is appropriate for these layered Fe-As systems. The observation of superconductivity despite a strong in-layer disorder puts also a strong constraint on the possible superconducting order parameters. While finalizing our investigation, Sefat *et al.* [8] and Wang *et al.* [9] reported the observation of superconductivity in Co doped LaFeAsO with a maximum $T_c \approx 10$ K. While their results support our analysis, the higher T_c observed in $\text{SrFe}_{2-x}\text{Co}_x\text{As}_2$ establishes much stronger evidence.

Samples were prepared by a sintering technique in glassy-carbon crucibles which were welded into tantalum containers and sealed into evacuated quartz tubes for heat treatment at 900°C for 16 h followed by two re-grinding and compaction steps. First precursors SrAs , Co_2As and Fe_2As were synthesized from elemental powders sintered at 600°C for 48 h (Fe, Co powder, 99.9 wt.%; As sublimed lumps 99.999 wt.%; Sr 99.99 wt.%). These educts were then powdered, blended in stoichiometric ratios, compacted, and heat treated. All steps were carried out within an argon-filled glove box (O_2 , $\text{H}_2\text{O} < 1$ ppm). This mode of synthesis helps to prevent possible contamination by toxic arsenic [10]. Samples were obtained in the form of sintered pellets.

Metallographic preparations and microstructure investigation on polished surfaces with optical microscopy were performed in an argon-filled glove box. Electron-probe microanalysis (EPMA) with energy dispersive analysis was accomplished in a Philips XL30 scanning electron microscope. Powder X-ray diffraction was performed using Co $K\alpha_1$ radiation ($\lambda = 1.789007 \text{ \AA}$) apply-

ing the Guinier Huber technique with LaB₆ as internal standard ($a = 4.15692 \text{ \AA}$). Crystallographic calculations were done with the WinCSD program package [11].

Evaluation of the lattice parameters and EPMA investigations of selected samples unambiguously reveals the substitution of Fe by Co which is accompanied by a decrease of the c axis length of the unit cell (see Table I). For the sample SrFe_{1.8}Co_{0.2}As₂ which was essentially single phase (minor impurity SrAs) the crystal structure was refined by Rietfeld methods (BaAl₄-type of structure [12], space group $I4/mmm$, Sr in $2a$ (0, 0, 0), Fe/Co in $4d$ (0, 1/2, 1/4), As in $4e$ (0, 0, 0.3613(1)); $R_I = 7.4$, $R_P = 10.1$). Other samples of this investigation contained as minor impurity phases Fe_{1-x}Co_xAs.

Magnetization was measured from 1.8–400 K in a SQUID magnetometer in various fields both after zero-field cooling (zfc) and during cooling in field (fc). Heat capacity was determined by a relaxation-type method on a commercial measurement system (1.9–100 K, 0–9 T). Electrical dc resistivity data $\rho(T)$ (3.8–320 K) were collected with a current density of $< 1 \times 10^{-3} \text{ A mm}^{-2}$ in a four contact arrangement. Due to the sample geometry the inaccuracy in ρ is estimated to be $\pm 20\%$.

To investigate the influence of electron doping on the electronic structure of SrFe₂As₂ on a microscopic level, we performed density functional band structure calculations within the local (spin) density approximation (L(S)DA). Using the experimental structural parameters [4], we applied the full-potential local-orbital code FPLO [13] (version 7.00-28) with the Perdew-Wang exchange correlation potential [14] and a carefully converged k -mesh of 24^3 points for the Brillouin zone. The substitution of Fe by Co and Sr by La was simulated within the virtual crystal approximation (VCA).

TABLE I: Lattice parameters a, c of SrFe_{2-x}Co_xAs₂ (nominal compositions) and superconducting transition temperature T_c^{mag} (defined as the crossing of the tangent to the steepest slope of the fc transition with $\chi = 0$), χ_0 is the high-field susceptibility at $T=0$. Data for $x=0$ are from Ref. [4].

x	a (\AA)	c (\AA)	T_c^{mag} (K)	χ_0 (10^{-6} emu/mol)
0.00	3.924(3)	12.34(1)	–	–
0.10	3.9291(1)	12.3321(7)	–	n.a.
0.15	3.9272(1)	12.3123(5)	<1.8	+780
0.20	3.9278(2)	12.3026(2)	19.2	+600
0.25	3.9296(2)	12.2925(9)	18.1	(+850)
0.30	3.9291(2)	12.2704(8)	13.2	+460
0.40	3.9293(1)	12.2711(7)	12.9	+360
0.50	3.9287(2)	12.2187(9)	<1.8	n.a.
1.00	3.9618(1)	11.6378(6)	–	n.a.

The magnetic susceptibility in a nominal field $\mu_0 H =$

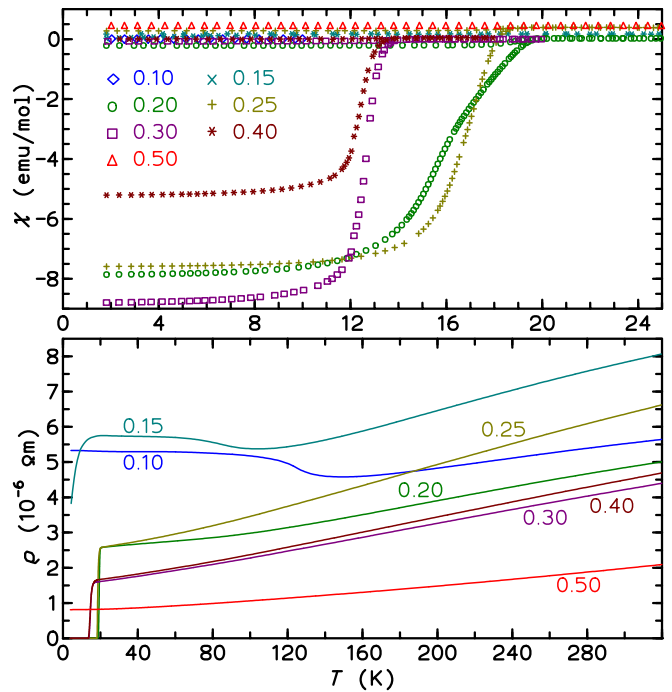


FIG. 1: (Color online) Top: magnetic susceptibility $\chi(T)$ of SrFe_{2-x}Co_xAs₂ samples in a nominal field of $\mu_0 H = 2 \text{ mT}$. Bottom: electrical resistivity of the same samples.

2 mT (Fig. 1 top) displays strong diamagnetic signals in zfc due to superconducting transitions in the $x=0.2-0.4$ samples with onset temperatures T_c^{mag} up to 19.2 K for $x=0.2$ (see Table I). The compounds with $x=0.1$ and $x=0.5$ show no traces of superconductivity. Even for this low external field the transitions are slightly rounded which indicates that the samples are not fully homogeneous. While the shielding signal (zfc) corresponds to the whole sample volume (considering approximate demagnetizing factors), the Meissner effect (fc) is much smaller, which is probably due to strong pinning.

The normal-state susceptibilities of the samples $x=0.2, 0.3,$ and 0.4 are field-independent for $T > 200 \text{ K}$. There, the compounds display a paramagnetism which can be described by $\chi(T) = \chi_0 + \chi_2 T^2$. The extrapolated χ_0 values are given in Table I. Diamagnetic core contributions are comparatively small ($\approx -50 \times 10^{-6} \text{ emu/mol}$). Due to the current sample quality some caution is necessary in interpreting χ_0 , but the order of magnitude and the temperature dependence is typical for an enhanced Pauli paramagnet. Comparing the χ_0 values with the electronic density of states at the Fermi level obtained from band structure calculations (see below) suggests an enhanced Sommerfeld-Wilson ratio, which decreases with increasing Co content for $x \geq 0.15$, in accordance with a magnetic instability for $x \leq 0.15$. SrCo₂As₂ is a Curie-Weiss paramagnet ($\mu_{\text{eff}} = 2.06 \mu_B/\text{f.u.}$, $\theta_{\text{CW}} = -29 \text{ K}$) and does not show magnetic ordering above 1.8 K.

The temperature dependence of the resistivity $\rho(T)$

(Fig. 1 bottom) at high temperatures is generally that of a bad metal. $\rho(300\text{ K})$ decreases gradually with electron doping from $5.5\text{--}8.0\ \mu\Omega\text{ m}$ for $x=0.10\text{--}0.15$ to $2.0\ \mu\Omega\text{ m}$ for $x=0.50$, as also observed for K-substituted samples.[3] For $x=0.10$ a stepwise increase of $\rho(T)$ is observed below $\approx 130\text{ K}$ which shifts to $\approx 90\text{ K}$ for $x=0.15$. This anomaly can be assigned to the afm ordering and the related lattice distortion observed at $T_0=205\text{ K}$ in SrFe_2As_2 [4, 5]. Thus, Co substitution (electron doping) leads to the suppression of the afm order in a similar way as reported for the K-substitution (hole doping) [15]. For $x=0.20$ no such anomaly is seen and the compound shows a superconducting transition at 19.4 K .

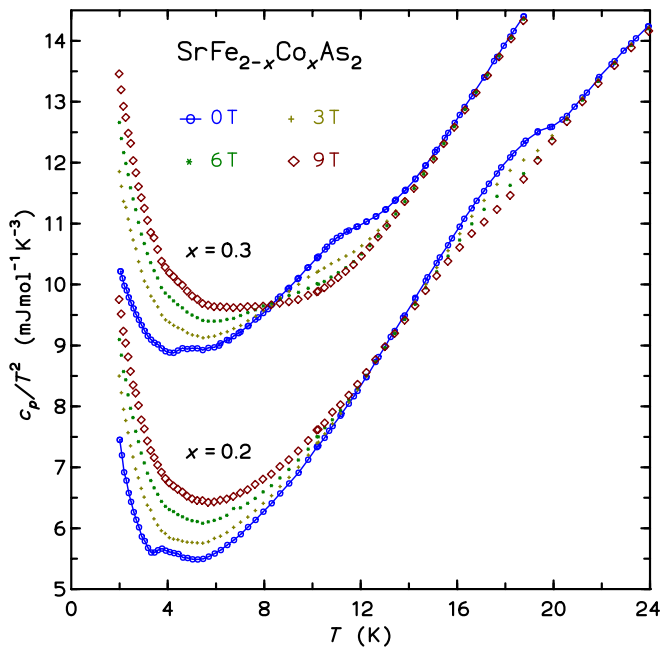


FIG. 2: (Color online) Molar isobaric specific heat c_p/T^2 of $\text{SrFe}_{2-x}\text{Co}_x\text{As}_2$ samples ($x=0.2$; $x=0.3$ shifted up by 3 units) for different magnetic fields. For better distinction the data for $\mu_0 H = 0$ are connected by a line.

In Fig. 2 the specific heat $c_p(T)$ for two selected samples is presented in a $c_p(T)/T^2$ versus T plot. Strongly rounded anomalies with onset at T_c as determined by $\rho(T)$ and $\chi(T)$ data are clearly visible confirming that the superconductivity is a bulk phenomenon in these samples. The idealized step heights Δc_p and the transition temperatures T_c^{cal} were evaluated by a fit with a phononic background and an electronic contribution according to the BCS theory or the phenomenological two-liquid model which applies well to the thermodynamic properties of some strong coupling superconductors. The model is convoluted with a Gaussian to simulate the broadening due to the chemical inhomogeneities.

$\Delta c_p/T_c^{\text{cal}}$ is $\approx 10\text{ mJ mol}^{-1}\text{ K}^{-2}$ for $x=0.2$ and $\approx 13\text{ mJ mol}^{-1}\text{ K}^{-2}$ for $x=0.3$. Interestingly, well below T_c the specific heat can still be described with a linear plus a

T^3 Debye lattice term, i.e. $c_p(T) = \gamma'T + \beta T^3$. While β is field-independent and corresponds to a lattice term with initial Debye temperature $\Theta_D(0) = 255(2)\text{ K}$ for both $x=0.2$ and 0.3 , the linear term γ' increases nearly linearly with field. For $x=0.2$ the values of γ' range from 12.6 mJ mol^{-1} at $\mu_0 H = 0\text{ T}$ to 17.5 at 9 T . Whether the residual γ' is induced by defects (see e.g. Ref. [16]) or whether it is an intrinsic contribution due to ungapped parts of the Fermi surface [17] has to be elucidated by further experiments. While we cannot make a definite statement on the superconducting coupling strength the better fit is obtained for $x=0.2$ and the two-fluid model while for $x=0.3$ the BCS fit is superior. This might indicate a variation of the coupling strength with Co content.

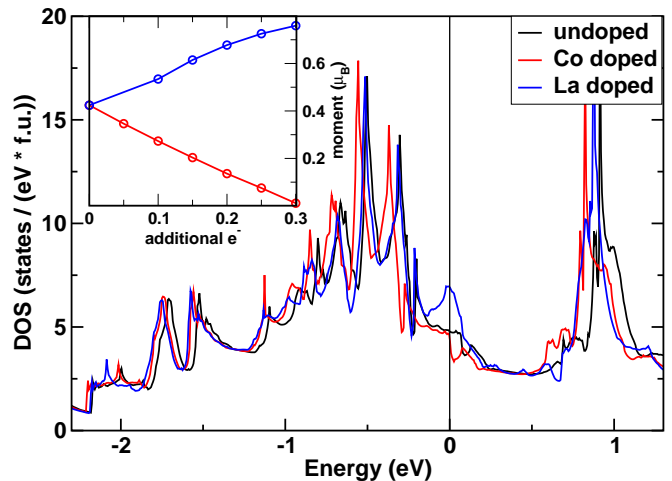


FIG. 3: (Color online) Total electronic densities of states for SrFe_2As_2 (black), $\text{SrFe}_{1.7}\text{Co}_{0.3}\text{As}_2$ (red) and the fictitious $\text{Sr}_{0.7}\text{La}_{0.3}\text{Fe}_2\text{As}_2$ (blue) in the vicinity of the Fermi level. Inset: dependence of the magnetic moment on the number of additionally doped electrons per formula unit for doping at the Fe site (red) and at the Sr site (blue), respectively.

For a microscopic study of the influence of doping with electrons on the electronic structure in the vicinity of the Fermi level ε_F , we simulated two different kinds of partial constituent exchange: (i) Co substitution at the Fe site and (ii) a fictitious La substitution at the Sr site to study possible differences for doping (i) within and (ii) outside the FeAs layers. Throughout all calculations we used the experimental lattice parameters [4] of the undoped SrFe_2As_2 to separate the influence of geometry changes and pure electronic doping effects. Since the changes of the lattice parameters upon doping are very small (see Table I) this approach is well justified. The resulting total density of states (DOS) for the Fe-3d dominated regions of the valence band for $\text{SrFe}_{2-x}\text{Co}_x\text{As}_2$ and $\text{Sr}_{1-x}\text{La}_x\text{Fe}_2\text{As}_2$, respectively, is shown in Fig. 3 for an exemplary doping level of $x=0.3$.

The two kinds of doping result in a rather different behavior. Whereas (i) Co doping on the iron site results in an almost perfectly rigid shift of the DOS for all studied

doping levels between $x=0$ and $x=0.5$, (ii) exchange of Sr by La can't be described at all in a rigid band picture in the vicinity of ε_F (see Fig. 3). In the case of Co substitution, a detailed analysis of the orbital-resolved DOS, the corresponding bands and band characters shows that the rigid band picture holds even for the individual orbitals close to ε_F . In contrast, the substitution (ii) of Sr by La shifts down the energy and changes the dispersion of a band with Fe-As-Sr hybrid character in a way that it gets partially occupied, whereas other bands remain basically unchanged. In consequence, this leads to the formation of a quite pronounced peak at ε_F and a sizable increase of the DOS (see Fig. 3). In general, from the experimental results for the $R\text{FeAsO}$ and the $A\text{Fe}_2\text{As}_2$ compound family it seems that the appearance of superconductivity at low temperatures is intrinsically related to the prior destruction of the spin density wave. Therefore, we studied the instability towards magnetism depending on the doping level for both doping scenarios (i) and (ii). In Fig. 3 we plot the size of the ordered Fe moment corresponding to the minimum in total energy in the VCA-LSDA calculations as a function of Co or La substitution. (ii) While La substitution stabilizes the magnetic state, electron doping by (i) Co leads to the disappearance of the magnetic ground state at $x=0.3$.

The disappearance of the magnetic instability is intimately connected with the occupation of the Fe- $3d_{x^2-y^2}$ related band along the Γ -Z direction as previously demonstrated [4] for the undoped compound (depending on the As z position). For $x=0.3$ (see Fig. 3) the related band edge is situated right at ε_F , leading to a reduced DOS and thus to the destruction of the magnetic state. In contrast, the tendency towards magnetism would be increased for (ii) La substitution. The DOS enhancement upon La substitution might lead to an instability of the $\text{Sr}_{1-x}\text{La}_x\text{Fe}_2\text{As}_2$ phase, which could be the reason why such compositions have not yet been reported.

The non-magnetic ground state for $x \leq 0.3$ in $\text{SrFe}_{2-x}\text{Co}_x\text{As}_2$ in the VCA-LSDA calculations is in surprisingly good agreement with the experimentally observed suppression of the magnetic state and the onset of superconductivity for $x=0.2$. In fact, the used VCA should result in an overestimate of the stability of a magnetic ground state since it does not include the direct influence of disorder in the Fe-As layer. Most likely, the doped Co impurities are in a non-magnetic state, indicated by calculations for SrCo_2As_2 that yield a non magnetic ground state in agreement with our measurements. Thus, a more sophisticated treatment of the Co impurities should lead to a sizable reduction of the critical concentration x for the suppression of the magnetic instability, in line with our experimental results.

In summary, we synthesized polycrystalline $\text{SrFe}_{2-x}\text{Co}_x\text{As}_2$ samples and investigated how electron doping within the Fe-As layers affects the magnetic and electronic properties of this kind of compounds. We

found that Co substitution suppresses the afm transition and the associated lattice distortion quite rapidly, from $T_0 = 205\text{ K}$ at $x=0$ to $T_0 \approx 90\text{ K}$ at $x=0.15$. For $x=0.2$ afm order is destroyed and bulk superconductivity with a $T_c \approx 20\text{ K}$ appears. Further increase of the Co content leads to a reduction of T_c and finally to the disappearance of superconductivity for $x \leq 0.5$. Thus electron doping within the Fe-As layer by substituting Co for Fe has a similar effect as hole doping in-between the layers by substituting K for Sr, or as electron doping by substituting F for O in LaFeAsO .

The observation of superconductivity upon substitution on the $3d$ site in the layered Fe-As systems is in strong contrast to the behavior in cuprates, where substitution on the Cu site lead to a fast suppression of superconductivity. This indicates that the suggested analogy between HTSC in cuprates and in Fe-As systems is not appropriate. Instead we observe a rigid-band like shift of the DOS to lower energy upon Co substitution. The suppression of the afm state, which occurs in the calculations at $x=0.3$, is connected with the $d_{x^2-y^2}$ states being pushed below the Fermi level. In contrast electron doping by substituting La for Sr leads in the calculation to a change in the dispersion and energy of a Fe-As-Sr hybrid band. The resulting increase of the DOS at ε_F stabilizes the afm state and might induce an instability of the SrFe_2As_2 phase. The nice correspondence between the experiments and VCA-LSDA band structure calculations indicates that an approach based on itinerant, weakly correlated $3d$ electrons is more appropriate for the description of the Fe-As systems than an approach based on localized $3d$ moments within a Hubbard model.

We thank U. Burkhardt, T. Vogel, R. Koban, K. Kreutziger, Yu. Prots, and R. Gumenuik for assistance.

-
- [1] Y. Kamihara, T. Watanabe, M. Hirano, and H. Hosono, *J. Am. Chem. Soc.* **130**, 3296 (2008).
 - [2] C. de la Cruz et al., *Nature* **453**, 899 (2008).
 - [3] M. Rotter, M. Tegel, I. Schellenberg, W. Hermes, R. Pöttgen, and D. Johrendt (2008), arXiv:0805.4021.
 - [4] C. Krellner, N. Caroca-Canales, A. Jesche, H. Rosner, A. Ormeci, and C. Geibel (2008), arXiv:0806.1209v1.
 - [5] M. Tegel, M. Rotter, V. Weiss, F. M. Schappacher, R. Pöttgen, and D. Johrendt (2008), arXiv:0806.4782v1.
 - [6] M. Rotter, M. Tegel, and D. Johrendt (2008), arXiv:0805.4630v1.
 - [7] C. Wang et al. (2008), arXiv:0804.4290.
 - [8] A. S. Sefat et al. (2008), arXiv:0807.0823v1.
 - [9] C. Wang et al. (2008), arXiv:0807.1304v1.
 - [10] J. O. Nriagu, *Arsenic in the environment, human health and ecosystem effects, part II* (Wiley, 1994).
 - [11] L. G. Akselrud, P. Y. Zavaliy, Yu. Grin, V. K. Pecharsky, B. Baumgartner, and E. Wölfel, *Mater. Sci. Forum* **133-136**, 335 (1993).
 - [12] K. R. Andress and E. Alberti, *Z. Metallkde.* **27**, 126 (1935).

- [13] K. Koepnik and H. Eschrig, Phys. Rev. B **59**, 1743 (1999).
- [14] J. P. Perdew and Y. Wang, Phys. Rev. B **45**, 13244 (1992).
- [15] G. F. Chen et al. (2008), arXiv:0806.1209v1.
- [16] G. Triscone and A. Junod, in *Bismuth-based High-Temperature Superconductors*, edited by H. Maeda and K. Togano (Marcel Dekker, New York, 1996), pp. 33–74.
- [17] S. L. Drechsler et al., Physica B **329**, 1352 (2003).